

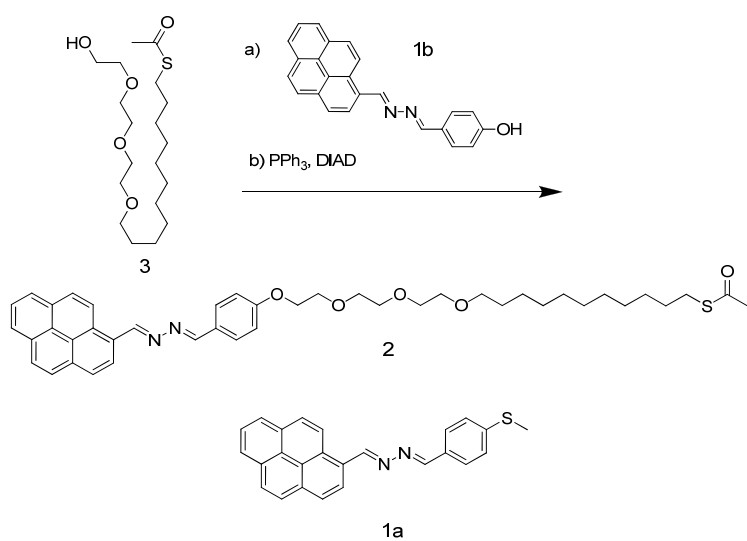
Selective Picomolar detection of mercury(II) using optical sensors

C. Díez-Gil, R. Martínez, I. Ratera, T. Hirsh, A. Espinosa, A. Tárraga, P. Molina, Otto S. Wolfbeis, J. Veciana*

Supplementary Information

SI 1. General procedure and synthesis:

All Chemicals were obtained from commercial suppliers and used without further purification. All organic solvents used on the synthesis of the products were distilled over sodium prior to use. Column chromatography purifications were performed on silica gel (35–70 µm). SPR slides substrates were purchased to SSens (Hengelo, Netherland). NMR spectra were recorded on a Bruker AV-400 spectrometer and referenced to SiMe₄ (δ in ppm and J in Hertz). NMR spectra were recorded at room temperature with CDCl₃ unless otherwise stated. Mass spectrometra were acquired on an Ultraflex MALDI-TOF (Matrix-Assisted Laser Desorption/Ionization-TOF) mass spectrometer (Bruker Daltonics, Billerica, MA). FT-IR-ATR spectra were realized on a FT-IR Spectrum One (Perkin Elmer, USA) using an Universal ATR sampling accessory. SPR measurements were carried out using a BIOSUPLAR 6 surface plasmon resonance spectrometer (Analytica-µ-Systems, Regensburg, Germany) working in Krestchmann mode.



Scheme 1 Synthesis of compounds **1a** and **2**.

General Procedure for the preparation of 1,4 unsymmetrically disubstituted 2,3-diaza-1,3-butadienes (1a and 1b). *n*-Butyllithium (1.6 M in hexane ; 0.70 ml) was dropped to a solution of *N*-(diethoxyphosphinyl)hydrazone of 1-pyrenecarboxaldehyde^[1] (0.410 g, 1.08 mmol) in dry THF (20 ml), at -78°C and in atmosphere of nitrogen. Then, a solution of the appropriate aldehyde (1.08 mmol) in dry THF (10 ml) was added dropwise and the mixture was stirred for 30 min. The reaction mixture was allowed to reach room temperature and stirred overnight. The solvent was evaporated under reduced pressure and the resulting solid was slurried with diethyl ether (25 ml) to give the corresponding disubstituted 2,3-diaza-1,3-butadienes **1** which were recrystallized from dichloromethane/diethyl ether (1/10).

1-(*p*-Methylthiophenyl)-4-(1-pyrenyl)-2,3-diaza-1,3-butadiene (1a): 85%. Mp: 224-226°C.

IR (Nujol), ν (cm⁻¹): 1614, 1594, 1245, 1068, 962, 848, 804, 719. ¹H NMR (CDCl₃): δ 2.52 (s, 3

H), 7.30 (d, J = 8.3 Hz, 2H), 7.81 (d, J = 8.3 Hz, 2H), 8.00 (t, J = 7.6 Hz, 1H), 8.06 (d, J = 8.8 Hz, 1H), 8.12 (d, J = 8.8 Hz, 1H), 8.20-8.22 (m, 4 H), 8.69 (d, J = 8.1 Hz, 1H), 8.78 (s, 1 H), 8.87 (d, J = 9.29 Hz, 1H), 9.69 (s, 1 H). ¹³C NMR (CDCl₃): δ 15.1, 122.7, 124.6, 124.9, 125.0, 125.8, 125.9, 126.1, 126.2, 126.2, 126.6, 127.4, 128.9, 130.5, 130.6, 130.7, 131.2, 133.4, 143.1, 160.7, 161.9. EIMS, m/z (%): 378 (M⁺, 85), 227 (72), 201 (100), 150 (15), 137 (22). Anal. Calc. for C₂₅H₁₈N₂S: C, 79.33; H, 4.79; N= 7.40. Found: C, 79.55; H, 4.56; N, 7.55.

1-(*p*-Hydroxyphenyl)-4-(1-pyrenyl)-2,3-diaza-1,3-butadiene (1b): 55%. Mp: 238-240 °C. IR

(Nujol), ν (cm⁻¹): 3399, 1605, 1270, 1164, 1107, 960, 878, 845, 825, 719. ¹H NMR (CDCl₃): δ

6.89 (d, J = 8.36 Hz, 2H), 7.80 (d, J = 8.36 Hz, 2 H), 8.13 (t, J = 7.68 Hz, 1H), 8.24 (d, J = 8.86 Hz, 1H), 8.30 (d, J = 8.82 Hz, 1H), 8.34-8.40 (m, 4 H), 8.69 (d, J = 8.09 Hz, 1 H), 8.79 (s, 1 H), 9.12 (d, J = 9.31 Hz, 1 H), 9.66 (s, 1 H). ¹³C NMR (CDCl₃): δ 116.2, 137.7, 124.1, 124.6, 124.8, 125.6, 126.4, 126.7, 126.9, 127.1, 127.2, 127.8, 129.3, 129.4, 130.0, 130.6, 131.0, 131.2, 133.0, 159.7, 162.0, 162.4. EIMS, m/z (%): 348 (M⁺, 100), 320 (23), 228 (68), 201 (77), 121 (6). Anal. Calc. for C₂₄H₁₆N₂O: C, 82.74; H, 4.63; N, 8.04. Found: C, 82.53; H, 4.90; N, 7.88.

Synthesis of 1-(4-alkoxyphenyl)-4-(1-pyrenyl)-2,3-diaza-1,3-butadiene derivative (2). Diisopropyl azodicarboxylate ((28 mg, 0.14 mmol, 27,6 μ l) was added dropwise to a solution

of triphenylphosphine (44.5 mg, 0.17 mmol), 1-(thioacetyl-undec-11-yl)tri(ethylene glycol)^[2] (100 mg, 0.14 mmol) and 1-(*p*-hydroxyphenyl)-4-(1-pyrenyl)-2,3-diaza-1,3-butadiene **1b** (50.6 mg, 0.14 mmol) in freshly distilled ether (20 ml). The mixture was stirred overnight at room temperature and the solvent was removed under reduced pressure. The yellow solid obtained was purified by column chromatography on silica gel, using ethyl ether as the eluent. Yield: 30%. R_f =0.8 (SiO₂; ethylether). Anal. Calcd. for C₄₃H₅₂N₂O₅S: C, 72.85; H, 7.39, N, 3.95, S

4.52. Found: C, 72.93; H, 7.51; N, 3.93; S 4.43. IR (ATR) ν (cm⁻¹): 3045, 2921, 2852, 1687,

1620, 1605, 1512, 1352, 1109. ¹H NMR (250 MHz, CDCl₃): δ 9.78-9.64 (m, 1H), 8.4 (d, J = 8.90 Hz, 1H), 8.82 (s, 1H), 8.73 (d, J = 8.72 Hz, 1H), 8.30-8.00 (m, 7H), 7.95-7.78 (m, 2H), 7.12-6.93 (m, 2H), 4.30-4.12 (m, 8H), 3.96-3.85 (m, 2H), 3.81-3.54 (m, 8H), 3.45 (t, J = 6.31, 6.31 Hz, 2H), 2.84 (t, J = 6.87, 6.87 Hz, 2H), 2.31 (s, 3H), 1.25 (s, 18H). ¹³C NMR (63 MHz, CDCl₃): δ 195.8, 161.7, 161.2, 159.9, 133.0, 131.0, 130.4, 130.1, 130.0, 128.6, 128.6, 127.2, 126.8, 126.6, 126.0, 125.9, 125.8, 125.6, 124.8, 124.7, 124.6, 122.5, 114.7, 71.3, 70.7, 70.4, 70.4, 69.8, 69.4, 67.3, 30.4, 29.4, 29.4, 29.3, 29.2, 29.1, 29.2, 28.9, 28.89, 28.59, 25.89; MS (MALDI-TOF) 709 (M⁺).

SI 2. Coverage study of compounds **1a** and **2** in a self assembled monolayer:

The use of redox-active probes to characterize the properties of SAMs has been extensively used in surface science.^[3] Thus, the barrier property and ionic permeability of modified electrodes were evaluated by studying the electron transfer reaction on the SAM-modified gold substrates using potassium ferro/ferri cyanide redox couple^[3c] The comparison between the relative intensities of the reduction/reoxidation peaks obtained for the bare gold surfaces and the thiol functionalized ones was then used to calculate the relative electrochemically accessible area of each sample.^[4] In order to analyze the structural organization of these monolayer films on Au surface, the following experiments were carried out immediately after the monolayer formation. The voltammetric measurements of the gold modified electrodes were recorded using a VersaSTAT 3 potentiostat (Princeton Applied Research, USA). A 1 mM of Fe(CN)₆³⁻, and a 0.1 M aqueous solution of KCl was used as electrolyte for the measurements. Clean gold and SAM modified electrodes were subjected to 5 potential cycles between 0.0 V and 0.6 V at a scan rate of 100 mV/s. In this case, the reversible peak associated with the ferro/ferri cyanide redox couple is only visible for the clean electrode, being almost completely neutralized for the thiol functionalized electrodes (Figure SI 1 top). Thus, it is possible to say that the monolayers

act as an insulator, limiting the approach of the redox molecules to the electrode surface and decreasing, therefore, the rate of electron transfer.

Results obtained for the two freshly prepared SAMs are shown in Figure SI 1. While the desorption of the SAM containing compound **1a** (Figure SI 1 left) reaches the 22% after 10 min, and the 100 % after only 30 min, data obtained for the monolayer of compound **2** (Figure SI 1 right), indicate no desorption even after 30 min of exposure. Thus, it is possible to establish that the SAM containing compound **2** not only depicts a better packing over the gold surface but also that its stability vs. the mercury mediated desorption is much higher.

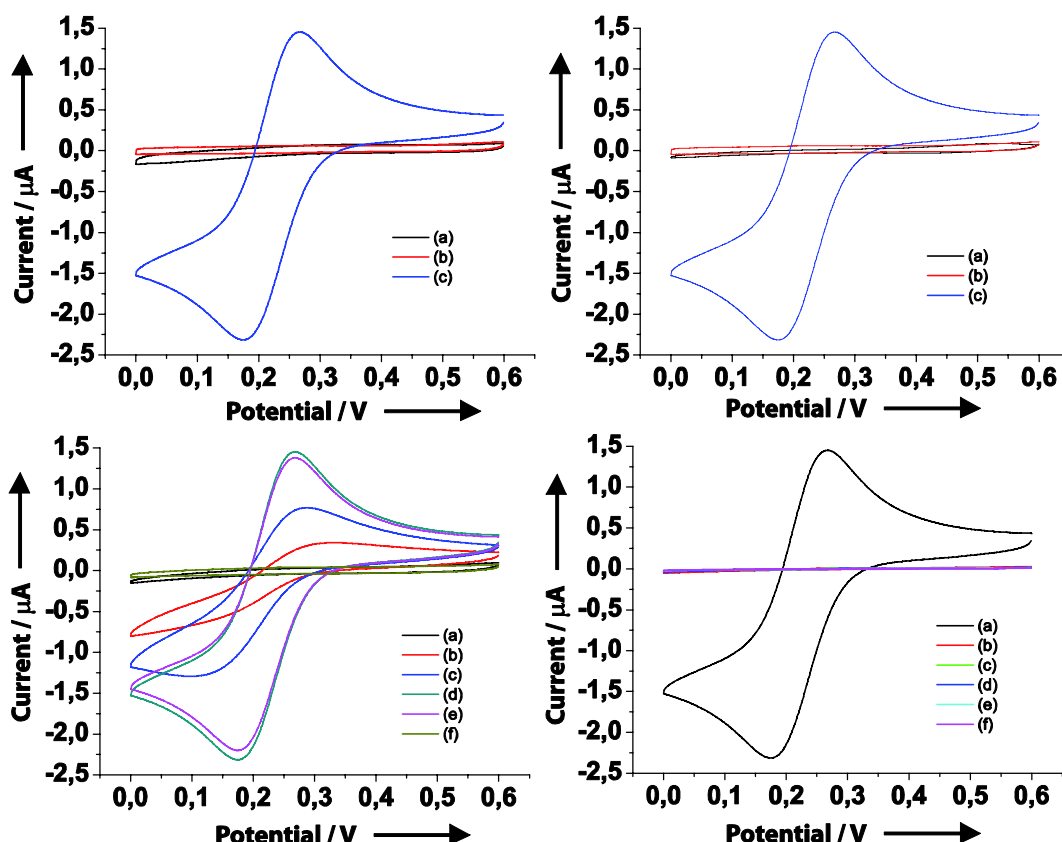


Figure SI 1 (top) Cyclic voltammograms of 1 mM $\text{K}_4\text{Fe}(\text{CN})_6$ in 0.1 M KCl aqueous solution using compound **1a** and **2**, up-left and up-right respectively, functionalized gold electrodes as working electrode. Cyclic voltammograms of 10^{-5}M $\text{Hg}(\text{ClO}_4)_2$, 1 mM $\text{K}_4\text{Fe}(\text{CN})_6$ in 0.1 M KCl aqueous solution at (a) a bare gold slide and compound **2** and **1a** (bottom-right and bottom-left, respectively) SAMs over gold for (b) $t = 0$ min (c) $t = 1$ min (d) $t = 10$ min (e) $t = 20$ min (f) $t = 30$ min. Scan rate: 100 mV s⁻¹.

SI 3. Contact angle studies:

Static and dynamic contact angles of freshly prepared self assembled monolayers (SAMs) of

compounds **1a** and **2**, before and after being in contact with mercury(II) ions ($0.1\mu\text{M}$ $\text{Hg}(\text{ClO}_4)_2$

(aq) solution) for 3 h, were determined with a OCA 15+ (Dataphysics, Germany) contact angle goniometer equipped with a motorized pipette. Data treatment and angle determination were carried out with the software SCA20 (Dataphysics, Germany). After being in contact with $\text{Hg}(\text{ClO}_4)_2$ solution, the SAMs were carefully rinsed with MilliQ water in order to remove any non bonded mercury salts. Three sets of advancing and receding angles, each at a different spot on each sample, were measured and averaged.

Results obtained for the dynamic contact angle measurements indicate the existence of a higher hysteresis, that might be related with a worse monolayer packing, in the case of the monolayer of compound **1a**, if compared with these obtained for compound **2**.

Table 1. Advancing (Avd), receding (Red) and static contact angles (in $^\circ$) of SAMs containing compounds **1a** and **2**, before and after being in contact with mercury (II) ions.

SAM	Before		After	
	Adv/Red	Static	Adv/Red	Static
1a	96 \pm 3/64 \pm 4	97 \pm 1	73 \pm 4/64 \pm 4	75 \pm 1
2	94 \pm 4/76 \pm 2	92 \pm 1	68 \pm 1/53 \pm 2	71 \pm 2

SI 4. XPS measurements:

XPS measurements were conducted on a X-ray photoelectron spectrometer PHI ESCA-5500 using monochromatic Al KR radiation (1486.6 eV, 300 W) for excitation. Freshly prepared samples were transferred to the XPS main chamber. The Au 4f7/2 signal was used as internal reference to correct the spectra for charging. The background was subtracted using the Shirley method in all spectra. Data analysis was performed by the acquisition software (MultiPak V6.1A, June 16, 1999, copyright Physical Electronics Inc., 1994-1999). The spectra were deconvoluted by fitting the spectral profiles with a series of symmetrical Gaussian envelopes after subtraction of the background.

X-ray photoelectron spectroscopy (XPS) (See Fig. SI 2) reveals signals for C 1s (corresponding to the C-C and C-H bonds and N 1s signals, which appear at 284.8 and 398 eV, respectively. A careful deconvolution of the C 1s peak reveals the existence of a shoulder at higher binding energy (286.3 eV) corresponding to the aromatic carbons of the receptor, and another peak (at 288.7 eV) that can be assigned to the carbon-heteroatom bonds. XPS also allowed us to follow the mercury recognition by the receptor unit. Thus, a freshly prepared SAM of compound **2** was

immersed for two hours into an aqueous $10\mu\text{M}$ solution of $\text{Hg}(\text{ClO}_4)_2$, rinsed with MiliQ water,

and dried with a stream of nitrogen. The XPS measurements showed that the peaks related to the C 1s were not affected by mercury(II) ions, but that the N 1s spectrum revealed a small shoulder at higher binding energies, (400.9 eV) characteristic of a N atom that is complexing a metal ion. This observation is in line with the appearance of two peaks at 100.2 and 104.4 eV corresponding to the Hg 5/2 f 7/2 f of the mercury(II).

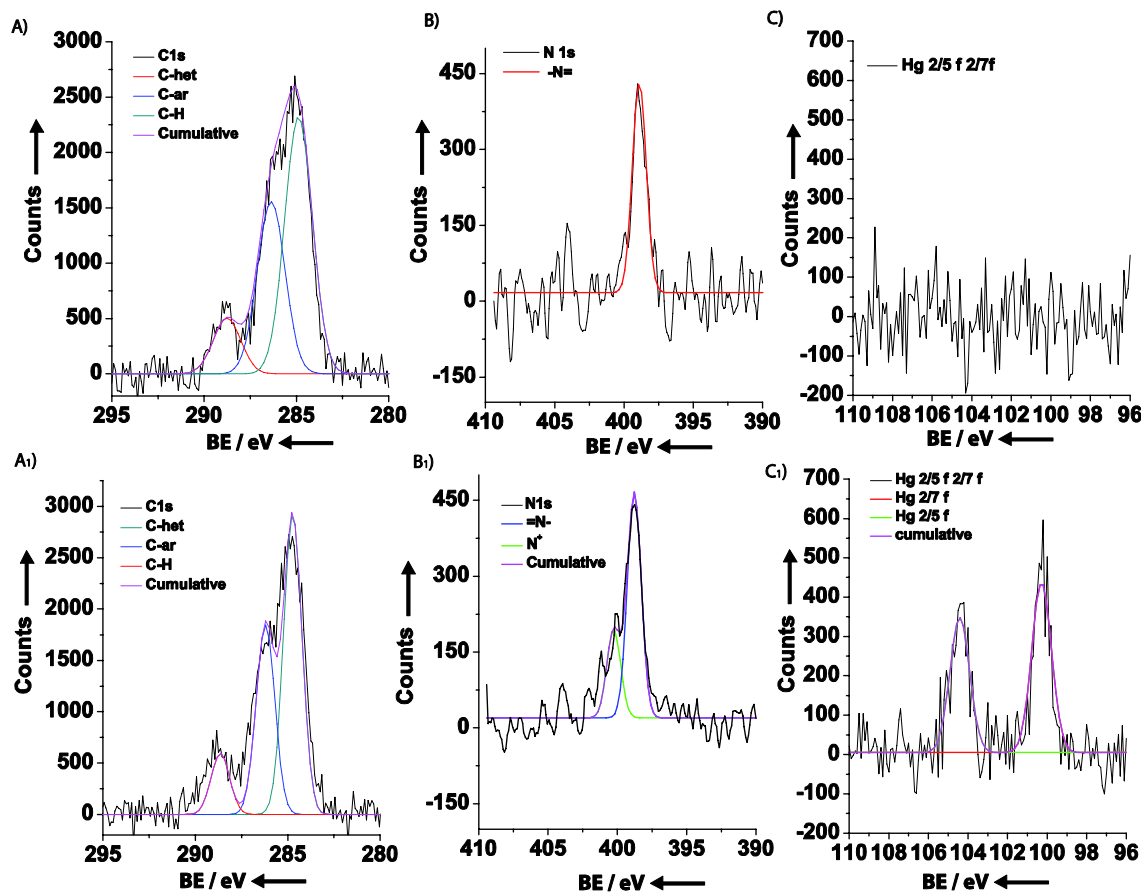


Figure SI 2. XPS spectra of compound **2** monolayer over a gold slide. A) C 1s peak deconvolution; B) N 1s corresponding peak; C) Hg 5/2 f 7/2 f spectra; A₁, B₁, and C₁ correspond to the C 1s, N 1s and Hg 5/2 f 7/2 f peaks after immersion for 2 h of the treated surface on an aqueous solution (10^{-5}M) of $\text{Hg}(\text{ClO}_4)_2$.

SI 5. SAMDI-ToF:

Gold surfaces functionalized with a monolayer of compound **2** were mounted on the MALDI-TOF analysis plate using double sized scotch tape. Mass analysis of the organic receptor self assembled monolayers was performed on a Ultraflex MALDI-TOF (Matrix-Assisted Laser Desorption/Ionization-TOF) mass spectrometer (Bruker Daltonics, Billerica, MA) in reflectron

positive ion mode. Each spectrum represents the average of 400 shots. Data analysis was performed using the *m/z* analysis software (Freeware, Proteomics, LLC).

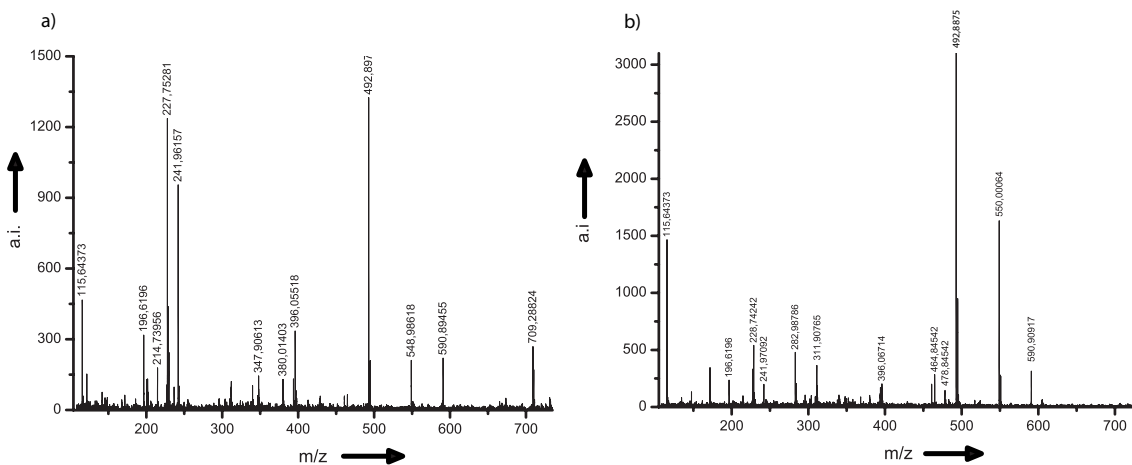


Figure SI 3. SAMDI-ToF spectra of a monolayer with compound **2** on a gold slide. a) Before treatment with $\text{Hg}(\text{ClO}_4)_2$; b) After treatment with an 10^{-3}M aqueous solution of $\text{Hg}(\text{ClO}_4)_2$.

SI 6. Theoretical calculations

6.1. Results

In order to get insight into the structural features of the above mentioned complexes, DFT quantum chemical calculations for suitable model systems have been performed using the Truhlar hybrid metafunctional mPW1B95^[5] (see Computational Details in 6.2) that has been recommended for general purpose applications. It was developed in order to produce a better performance where weak interactions are involved, such as those between ligands and heavy metals.^[6] At the working mPW1B95/6-31G**/StRSCcep level only a minimum for a *C*₁-symmetric 2:2 L_2Hg_2 complex was found (Figure SI-4 up) featuring two identical Hg atoms that are essentially linearly di-coordinated ($\text{L}-\text{Hg}-\text{L}'$ angle 176.5°) by the action of a pyrene C-10 atom ($d_{\text{C}-\text{Hg}} = 2.263 \text{ \AA}$, WBI = 0.402, $\rho(r_c) = 8.04 \cdot 10^{-2} \text{ e} \cdot a_0^{-3}$) in one ligand and a N atom belonging to the other ligand ($d_{\text{N1}-\text{Hg}} = 2.182 \text{ \AA}$, WBI = 0.364, $\rho(r_c) = 8.87 \cdot 10^{-2} \text{ e} \cdot a_0^{-3}$), being the other intraligand N···Hg²⁺ contact (below the sum of van der Waals radii) characteristic of a weak interaction ($d_{\text{N2}-\text{Hg}} = 2.623 \text{ \AA}$, WBI = 0.146, $\rho(r_c) = 3.60 \cdot 10^{-2} \text{ e} \cdot a_0^{-3}$). As a consequence of bonding to the metal, C-10 is pyramidalized as evidenced by the high value (34.0°) of the angle formed by the C10-H bond with the pyrene mean plane. Moreover a fourth coordination position around Hg is completed in the gas-phase optimized structure by a weaker anagostic type interaction^[7] with a phenyl *ortho*-H atom (angle_{C-H···Hg} = 122.0° , $d_{\text{Hg} \cdots \text{H}} = 2.700 \text{ \AA}$, WBI = 0.014, $\rho(r_c) = 1.28 \cdot 10^{-2} \text{ e} \cdot a_0^{-3}$). The intermetallic distance is large enough to account for no more than residual interaction ($d_{\text{Hg} \cdots \text{Hg}} = 4.166 \text{ \AA}$, WBI = 0.026, no BCP found). The resulting six-membered tetrazamercurycycle shows a *boat* type conformation with parallel N-N bonds, a

Hg1-N1-N2-Hg2 torsion angle of 39.0°, and an azine dihedral (-CH=N-N=CH-) of 49.1° (180° in the free ligand). Within every ligand, the pyrenyl and phenyl mean planes lie almost orthogonal (81.7°) to each other.

In the case of the 2:1 complex, two minima close in energy ($\Delta E = 5.34 \text{ kcal}\cdot\text{mol}^{-1}$) were located in the potential energy surface. The absolute minimum has a C_2 -symmetric structure with every L molecule in extended conformation (dihedral_{CH=N-N=CH} = 168.6°) mainly acting as six-membered *N,C*-chelates (angle_{N-Hg-C} = 76.8°). In contrast to the 2:2 stoichiometry, the 2:1 case features a strong N-Hg bond ($d_{N-Hg} = 2.278 \text{ \AA}$, WBI = 0.290, $\rho(r_c) = 7.41 \cdot 10^{-2} \text{ e}\cdot a_0^{-3}$), almost aligned with the C_2 -related bond (angle_{N-Hg-N} = 166.4°), supplemented up to the hexacoordination around the metal atom by weaker C-Hg ($d_{C-Hg} = 2.694 \text{ \AA}$, WBI = 0.064, $\rho(r_c) = 3.13 \cdot 10^{-2} \text{ e}\cdot a_0^{-3}$) and anagostic H···Hg interactions (angle_{C-H···Hg} = 119.0°, $d_{Hg\cdots H} = 2.590 \text{ \AA}$, WBI = 0.027, $\rho(r_c) = 1.61 \cdot 10^{-2} \text{ e}\cdot a_0^{-3}$), the later involving the imine protons (Figure SI-4 down).

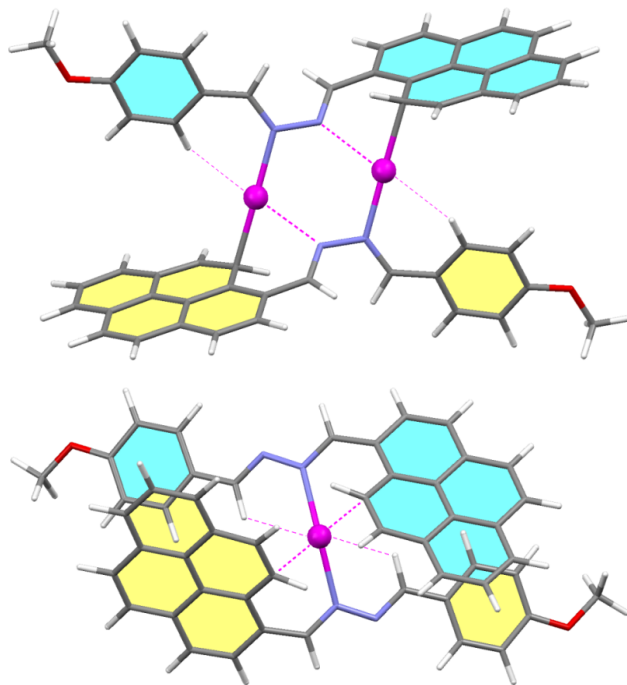


Figure SI-4: Calculated (mPW1B95/6-31G**/StRSC-ecp) structures for the 2:2 (up) and 2:1 (down) mercury (II) complexes, using the receptor core as model.

6.2. Computational Details

The reliably accurate description of weak interactions like hydrogen bonds and other found in supramolecular complexes generally requires a treatment of electron correlation. Density functional theory^[8] (DFT) has proved quite useful in this regard offering an electron correlation frequently comparable to the second-order Møller–Plesset theory (MP2) or in certain cases, and for certain purposes, even superior to MP2, but at considerably lower computational cost. Due to the size of the systems investigated in the present study the cost advantage that offers mPW1B95 method in comparison with MP2 was significant. Calculated geometries at the DFT

level were fully optimized in the gas-phase with tight convergence criteria using the Gaussian 03 package.^[9] The 6-31G** basis set was employed in the optimizations for all atoms except mercury, for which the Stuttgart relativistic small-core basis set (StRSC) with effective core potential (ecp)^[10] was used. From these gas-phase optimized geometries all reported data were obtained by means of single-point (SP) calculations at the mPW1B95/6-31G**/StRSC-ecp level. Energy values are uncorrected for the zero-point vibrational energy. Bond orders were characterized by the Wiberg's bond index^[11] (WBI) and calculated with the natural bond orbital (NBO) method as the sum of squares of the off-diagonal density matrix elements between atoms.

SI 7. Control SPR measurements

Control experiments were carried out using a freshly prepared monolayer compound **3** in order to maximize the similarity of the surfaces. Prior to the measurement the gold sensor chip was stabilized by exposing it to an aqueous solution with a controlled ionic strength (aqueous solution of NaCl 0.1 M) at a constant flux of 100 µL/min for 30 minutes in order to avoid effects of changing ionic strength. After addition of several solutions of mercury(II) ions of different concentrations (up to 10^{-7} M) in aqueous buffer, no signal was observed, indicating the lack of any unspecific adsorption (Figure SI-4).

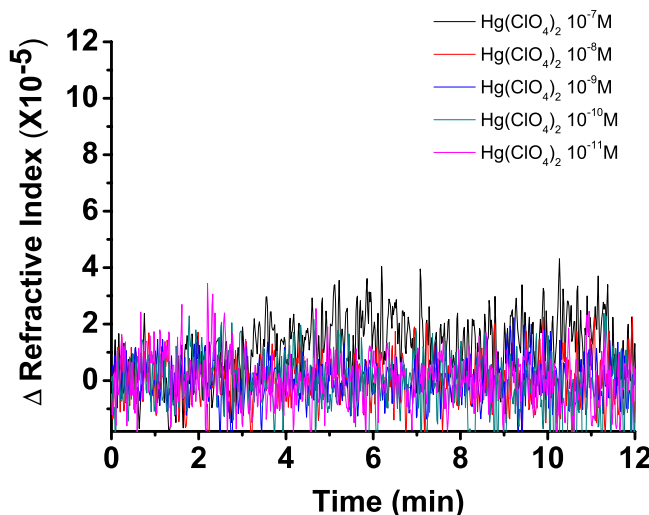


Figure SI-4: a) SPR sensogram upon addition of mercury(II) ions on a receptor **3** monolayer on a gold substrate.

SI 8. Regeneration tests of the SPR mercury(II) ion sensor

Regeneration test of a freshly prepared SPR sensor were developed in order to probe the reusability of the gold slide modified with SAMs of compound **2**.

The chip preparation and measurement procedure followed was the same as the one used for the sensor calibration. In this case a 10^{-10} M with a controlled ionic strength (0.1 M NaCl) aqueous solution of $\text{Hg}(\text{ClO}_4)_2$ was used as mercury source.

Alternating cycles of mercury and buffer solutions were pumped through the SPR system until a decrease on the observed mercury signal was observed. This happened after 4 cycles. Thus it is possible to conclude that, with the appropriate washing; it is possible to reuse our Hg^{2+} sensor up to four times without loss of sensitivity. A 48% of the initial SPR signal was loss after the fourth washing step, therefore this sensor was considered inappropriate for further Hg^{2+} analysis.

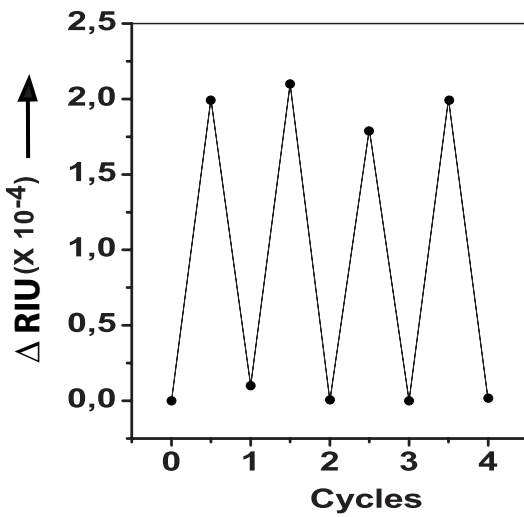
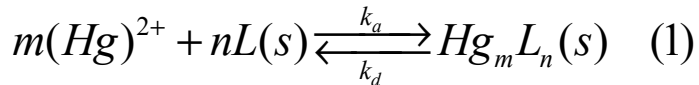


Figure SI-6: Regeneration assay with the compound **2** SAM functionalized sensor chip after mercury detection (mercury concentration used for the regeneration assay was 10^{-10}M).

SI 9. Binding Kinetics

A general reaction scheme is exploited in order to describe the function of this analytical system,



$$\frac{d[\text{Hg}_m L_n]}{dt} = k_a [\text{Hg}^{2+}]^m [L]^n - k_d [\text{Hg}_m L_n] \quad (2)$$

Where L is the receptor monolayer anchored to the Au surface, and $\text{Hg}_m L_n$ is the complex formed on the surface. The complex formation rate can be defined as equation (2), where $[\text{Hg}^{2+}]$ is the concentration of mercury ions present in the media, $[L]$ the concentration of ligand anchored to the surface and $[\text{Hg}_m L_n]$ the concentration of organometallic complex on the surface. Here the concentration of the complex ($[\text{Hg}_m L_n]$) can be approximated as the surface

coverage, which is proportional to the SPR signal (ΔRIU). Due to negligibly small concentration differences of analyte Hg^{2+} during complexation, concentration $[\text{Hg}^{2+}] = C$ is assumed to be constant in time. Therefore, complex formation is considered as pseudo first order kinetics in SPR biosensors,^[12] and equation 2 can be rewritten as 3 and rearranged in 4.

$$\frac{d\Delta\text{RIU}}{dt} = k_a C (\Delta\text{RIU}_{\max} - \Delta\text{RIU}_t) - K_d \Delta\text{RIU}_t \quad (3)$$

$$\frac{d\Delta\text{RIU}}{dt} = k_a C \Delta\text{RIU}_{\max} - (k_a C + k_d) \Delta\text{RIU}_t \quad (4)$$

Thus, Equation 4 can be regarded as a straight line:

$$\frac{d\Delta\text{RIU}}{dt} = -k_s \Delta\text{RIU}_t + b \quad \text{with} \quad k_s = (k_a C + k_d) \quad (5)$$

Parameters k_s and b can be determined by linear regression of a plot of $d\Delta\text{RIU}/dt$ vs. ΔRIU values (see Figure SI-5 b). The determined k_s value is a concentration-dependent parameter. This method is called the linearization method,^[13] because the data are presented in such a way, that the relevant parameter k_s can be determined by linear regression.

A closer look to Figure SI-5 a) shows that the adsorption of Hg^{2+} by the monolayer of receptor **2** follows a S-type adsorption behavior^[14] indicating the existence of a cooperative mechanism, that is reduced after approximately 6 min and totally finished after 18 min. The adsorption can, thus be divided into two different regions I and II. While in region I adsorption rate increases with coverage, in region II it follows Langmuir type kinetics, being this part the one chosen to perform the kinetic analysis of the system.

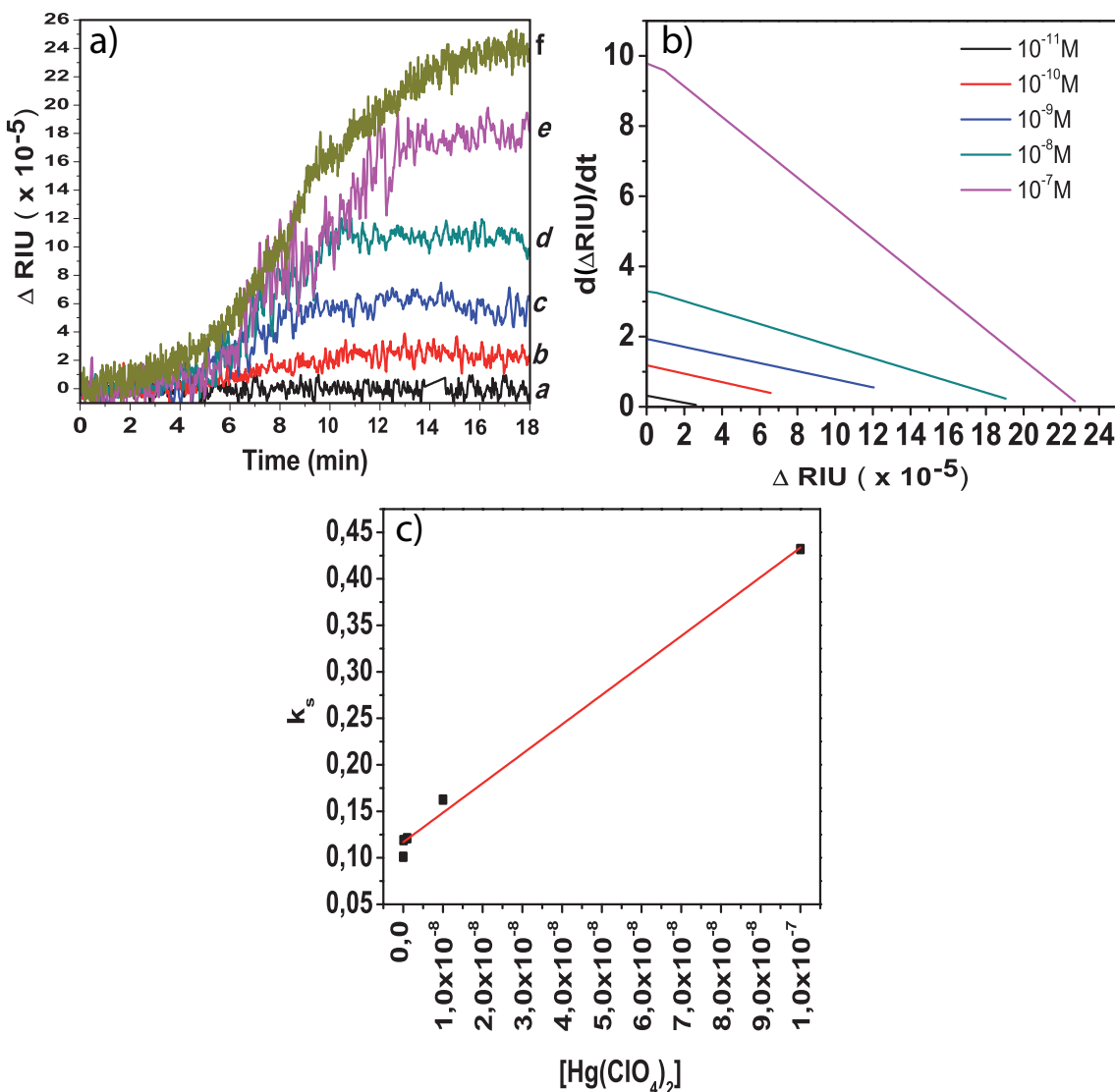


Figure SI-5: a) SPR sensogram upon addition of mercury(II) ions on a receptor **2** monolayer on a gold substrate; b) Calculated $d\Delta\text{RIU}/dt$ vs. ΔRIU representation; c) K_s vs. C of mercury(II) ions.

Kinetic rate constants are determined by a plot of k_s values vs. C (Fig. SI 5 c). Linear regression reveals the association rate constant from the slope of the plotted straight line, and the dissociation rate constant from the y-intercept of the plotted line.

K_d and K_a values obtained this way are 0.1168 s^{-1} and $3.16 \times 10^6 \text{ M}^{-1}\text{s}^{-1}$, respectively, in agreement with the ciphers obtained from solution studies for the same parameters.^[15] Linear fitting regression the fitting obtained is 0.996.

It is worthy to remark that this value is just an approximation of the kinetic constant involve in the recognition mechanism, and that supposes that all the SPR signal changes are due to the anchoring of mercury(II) to the receptor core, discarding the existence of other factors such as the appearance of fluorescence or a structural change on the monolayer.

Calculated structures: cartesian coordinates (in Å) and energies computed for model complexes $[L_2Hg_2]^{4+}$ and $[L_2Hg]^{2+}$.

Complex $[L_2Hg_2]^{4+}$: $E = -2600.53203042$ au

C	0.00000000	0.00000000	0.00000000	C	5.92360634	-0.90535991	-1.77674779
N	1.32048273	0.00000000	0.00000000	N	4.60312361	-0.90535991	-1.77674779
N	1.92776841	1.26688785	0.00000000	N	3.99583793	-2.17224776	-1.77674779
C	1.50385698	2.17313256	0.89476887	C	4.41974935	-3.07849247	-2.67151666
H	-0.51384306	0.96413959	-0.14384859	H	6.43744940	-1.86949952	-1.63289920
H	0.86493584	1.75534475	1.68572960	H	5.05867049	-2.66070467	-3.46247739
C	-0.84380698	-1.16877152	0.09154653	C	6.76741332	0.26341161	-1.86829433
C	-0.44147645	-2.43244420	0.61796709	C	6.36508279	1.52708429	-2.39471488
C	0.84058689	-2.63453952	1.31699105	C	5.08301945	1.72917961	-3.09373884
C	1.13212586	-3.90536308	1.91584174	C	4.79148048	3.00000316	-3.69258953
C	0.26798873	-5.00078686	1.79074093	C	5.65561761	4.09542695	-3.56748872
C	0.57194298	-6.25790032	2.39550199	C	5.35166336	5.35254041	-4.17224978
C	-0.34051296	-7.30317991	2.33042908	C	6.26411931	6.39782000	-4.10717687
C	-1.57040021	-7.11963693	1.67105978	C	7.49400656	6.21427701	-3.44780757
C	-1.92574865	-5.88826240	1.06944251	C	7.84935499	4.98290249	-2.84619030
C	-3.20280638	-5.70110593	0.44015064	C	9.12641272	4.79574602	-2.21689843
C	-3.55409246	-4.48238277	-0.08642073	C	9.47769880	3.57702287	-1.69032709
C	-2.65713812	-3.37056178	-0.02984349	C	8.58074445	2.46520188	-1.74690432
C	-3.03800519	-2.09063612	-0.49865039	C	8.96161153	1.18527623	-1.27809741
C	-2.16431057	-1.01998590	-0.42092069	C	8.08791690	0.11462601	-1.35582711
C	-0.99825980	-4.80442920	1.11799493	C	6.92186615	3.89906928	-2.89474274
C	-1.34802998	-3.53741101	0.55404201	C	7.27163634	2.63205109	-2.33078983
H	1.23667818	-1.76323835	1.86200493	H	4.68692816	0.85787844	-3.63875272
H	2.02750502	-3.99766993	2.53904132	H	3.89610133	3.09231002	-4.31578911
H	1.52106765	-6.38104398	2.92342807	H	4.40253869	5.47568407	-4.70017586
H	-0.11607071	-8.26216058	2.80043913	H	6.03967705	7.35680066	-4.57718692
H	-2.28549135	-7.94612420	1.63362711	H	8.20909768	7.04076429	-3.41037491
H	-3.90134755	-6.54018894	0.40644374	H	9.82495387	5.63482903	-2.18319154
H	-4.53640578	-4.34020295	-0.54166881	H	10.46001214	3.43484302	-1.23507901
H	-4.03868880	-1.95006395	-0.91251943	H	9.96229514	1.04470404	-0.86422837
H	-2.48309492	-0.03918000	-0.78244140	H	8.40670125	-0.86617991	-0.99430640
C	1.81552085	3.55239354	0.98533190	C	4.10808549	-4.45775345	-2.76207968
C	2.36228975	4.34690445	-0.07109157	C	3.56131659	-5.25226436	-1.70565622
C	2.63130033	5.68441430	0.11663334	C	3.29230601	-6.58977421	-1.89338113
C	2.35980654	6.30621808	1.37666209	C	3.56379979	-7.21157799	-3.15340988
C	1.78903197	5.54258153	2.43034376	C	4.13457437	-6.44794144	-4.20709155
C	1.51794557	4.20275914	2.22419964	C	4.40566076	-5.10811906	-4.00094742
H	2.48580674	3.92642077	-1.07509877	H	3.43779959	-4.83178069	-0.70164902
H	3.00640226	6.31735234	-0.68915490	H	2.91720407	-7.22271226	-1.08759288
H	1.55384890	6.00568439	3.38854024	H	4.36975743	-6.91104431	-5.16528803
H	1.07569191	3.62066320	3.03717437	H	4.84791442	-4.52602312	-4.81392215
O	2.64980632	7.59713572	1.43886198	O	3.27380002	-8.50249564	-3.21560976
C	2.36705446	8.35853945	2.64946725	C	3.55655188	-9.26389936	-4.42621503
H	2.69045961	9.37868723	2.42319564	H	3.23314672	-10.28404715	-4.19994343
H	2.94382362	7.95438581	3.49371974	H	2.97978272	-8.85974573	-5.27046753
H	1.28855936	8.34059059	2.86158434	H	4.63504697	-9.24595051	-4.63833213
Hg	2.40166036	-2.37094948	-0.29989709	Hg	3.52194598	1.46558956	-1.47685070

Complex $[L_2Hg]^{2+}$: **E = -2448.33791554 au**

Hg	0.0000000	0.0000000	0.0000000	C	-0.26920996	5.76745829	3.35604381
C	3.16995608	0.0000000	0.0000000	C	-1.19936495	5.26634879	2.42111408
N	2.12554211	0.81848483	0.0000000	C	-2.06911816	6.12837941	1.67273739
N	2.39467519	2.13464149	-0.17150125	C	-2.98268979	5.62136658	0.78148680
C	1.39247405	2.94197079	-0.40429775	C	-3.08170343	4.21240599	0.54716820
H	4.13144936	0.48065300	-0.21677014	C	-4.02330637	3.66538756	-0.35620620
H	0.35870092	2.52581775	-0.44924964	C	-4.05733610	2.30240880	-0.61059045
C	3.13674023	-1.43145707	0.14107666	C	-1.29205490	3.85102944	2.22505815
C	2.13619966	-2.15947912	0.86193536	C	-2.21182531	3.32193585	1.26750414
C	1.25304155	-1.53914268	1.82146377	H	-1.81488428	-0.01447743	1.97795811
C	0.25450291	-2.26406059	2.45147767	H	-0.16270785	0.89775722	3.57999065
C	0.06302898	-3.65466303	2.18562347	H	1.05033179	2.85122074	4.55138560
C	-0.96787644	-4.40446026	2.79625604	H	1.24640336	5.31809184	4.82910992
C	-1.06696002	-5.78019412	2.58019152	H	-0.19524566	6.84791309	3.50149267
C	-0.13296692	-6.43792375	1.77046230	H	-2.00545657	7.20579307	1.84350950
C	0.91930701	-5.73323087	1.14875485	H	-3.65697838	6.28809279	0.23911308
C	1.91063674	-6.39258235	0.34740842	H	-4.71864895	4.33251678	-0.87014763
C	2.93971089	-5.69301632	-0.23363934	H	-4.76015196	1.90607290	-1.34744702
C	3.04520772	-4.27324767	-0.08196120	C	-1.35015644	-4.00725018	-1.95860250
C	4.10303271	-3.53247648	-0.66005711	C	-2.60891241	-4.60507160	-2.25699030
C	4.14832619	-2.15072003	-0.54925072	C	-2.66954941	-5.84170887	-2.8649956
C	1.01256171	-4.31697003	1.33761202	C	-1.47442216	-6.52899594	-3.20921427
C	2.05748387	-3.57923707	0.69986985	C	-0.21619105	-5.95135310	-2.91668400
H	1.48947306	-0.52801270	2.17002429	C	-0.16707838	-4.70786646	-2.29796249
H	-0.37018231	-1.78613363	3.21270394	H	-3.52440939	-4.06971996	-1.99988149
H	-1.67840430	-3.89827478	3.45458828	H	-3.62232966	-6.31636966	-3.10400368
H	-1.86523208	-6.34973565	3.05903437	H	0.70815567	-6.46701814	-3.17600956
H	-0.20667668	-7.51795423	1.62176895	H	0.80474608	-4.25557707	-2.08298545
H	1.84316183	-7.47635316	0.22524427	O	-1.65150084	-7.71804250	-3.80859543
H	3.70242333	-6.21233192	-0.81839504	C	-0.49627375	-8.47097455	-4.22458717
H	4.88219431	-4.05987178	-1.21454779	H	-0.89252407	-9.37892537	-4.69064433
H	4.94772533	-1.59337101	-1.04353097	H	0.09712031	-7.90338633	-4.95831811
C	1.55387636	4.34686982	-0.63819371	H	0.12917473	-8.73995024	-3.35858007
C	2.83125515	4.97573719	-0.57718913				
C	2.95959240	6.32523692	-0.83214769				
C	1.81783889	7.10150287	-1.16828235				
C	0.54147213	6.49362628	-1.22963959				
C	0.42301540	5.13453676	-0.96443956				
H	3.70705159	4.37420112	-0.32823932				
H	3.92804037	6.82601723	-0.79285834				
H	-0.34233289	7.07687801	-1.48709469				
H	-0.56101215	4.66190372	-1.02386519				
O	2.06084849	8.40046229	-1.40931578				
C	0.96820464	9.25772631	-1.79106605				
H	1.41294328	10.24651157	-1.94308431				
H	0.50583719	8.90857137	-2.72751740				
H	0.21209701	9.30888130	-0.99157469				
C	-3.13182414	0.06356941	-0.48606382				
N	-2.08355994	-0.74849673	-0.53514235				
N	-2.29676466	-1.97141573	-1.07655394				
C	-1.25473345	-2.71234469	-1.35146699				
H	-4.03887421	-0.32632181	-0.96327543				
H	-0.23484850	-2.31934449	-1.12948404				
C	-3.14934582	1.41044240	0.01960543				
C	-2.28597302	1.90979328	1.04720989				
C	-1.54812739	1.04720772	1.93996422				
C	-0.67274055	1.56682038	2.87975327				
C	-0.47069201	2.97505165	3.01081404				
C	0.43914517	3.52301711	3.94342551				
C	0.54257843	4.90600228	4.10404511				

References

- [1] R. Martínez, I. Ratera, A. Tárraga, P. Molina, J. Veciana, *Chem. Commun.*, **2006**, *36*, 3809-3811.
- [2] a) C. Pale-Grosdemange, E. S. Simon, K. L. Prime, G. M. Whitesides, *J. Am. Chem. Soc.* **1991**, *113*, 12-20; b) A. G. Barrientos, J. M. de la Fuente, T. C. Rojas, A. Fernández, D. Penadés, *Chem. Eur. J.* **2003**, *9*, 1909-1921.
- [3] a) M. Geissler, J. Chen, Y. Xia, *Langmuir* **2004**, *20*, 6993-6997; b) R. Brito, R. Tremont, C. R. Cabrera, *J. Electroanal. Chem.* **2004**, *574*, 15-22; c) R. Brito, R. Tremont, O. Feliciano, C. R. Cabrera, *J. Electroanal Chem.* **2003**, *540*, 53-59.
- [4] M. Weisser, G. Nelles, P. Wohlfart, G. Wenz, S. Mittler-Neher, *J. Phys. Chem.* **1996**, *100*, 17893-17900.
- [5] a) Y. Zhao, D. G. Truhlar, *J. Phys. Chem. A*, **2004**, *108*, 6908-6918; b) Y. Zhao, D. G. Truhlar, *J. Phys. Chem. A* **2005**, *109*, 5656-5667.
- [6] For instance, see: Muñiz, J.; Sansores, L. E.; Martínez, A.; Salcedo, R. *J. Mol. Struct.* **2007**, *820*, 141-147.
- [7] Anagostic M–H–C bonds are best described as a “hydrogen bond” involving a 3-centre-4-electron orbital interaction with an electrostatic contribution in which the metal serves as a hydrogen bond acceptor. They are characterized by relatively long M···H distances (\approx 2.3–3.2 Å) and large M–H–C angles (\approx 110–170°). For recent reviews see: (a) Scherer, W.; McGrady, G. S. *Angew. Chem. Int. Ed.*, **2004**, *43*, 1782-1806. (b) M. Brookhart; M. L. H. Green; G. Parkin, *Proc. Natl. Acad. Sci. USA*, **2007**, *104*, 6908-6914.
- [8] (a) Becke, A. D.; *J. Chem. Phys.*, **1993**, *98*, 5648; (b) Lee, C.; Yang, W.; Parr, R. G. *Phys. Rev.*, **1998**, *B37*, 785; (c) Vosko, S. H.; Wilk, L.; Nusair, M. *Can. J. Phys.*, **1980**, *58*, 1200; (d) Stephens, P. J.; Devlin, F. J.; Chabalowskin, C. F.; Frisch, M. J.; *J. Phys. Chem.*, **1994**, *98*, 11623.
- [9] M. J. Frisch; G. W. Trucks; H. B. Schlegel; G. E. Scuseria; M. A. Robb; J. R. Cheeseman; J. A. Montgomery Jr.; T. Vreven; K. N. Kudin; J. C. Burant; J. M. Millam; S. S. Iyengar; J. Tomasi; V. Barone; B. Mennucci; M. Cossi; G. Scalmani; N. Rega; G. A. Peterson; H. Nakatsuji; M. Hada; M. Ehara; K. Toyota; R. Fukuda; J. Hasegawa; M. Ishida; T. Nakajima; Y. Honda; O. Kitao; H. Nakai; M. Klene; X. Li; J. E. Knox; H. P. Hratchian; J. B. Cross; C. Adamo; J. Jaramillo; R. Gomperts; R. E. Stratmann; O. Yazyev; A. J. Austin; R. Cammi; C. Pomelli; J. W. Ochterski; P. Y. Ayala; K. Morokuma; G. A. Voth; P. Salvador; J. J. Dannenberg; V. G. Zakrzewski; S. Dapprich; A. D. Daniels; M. C. Strain; O. Farkas; D. K. Malick; A. D. Rabuck; K. Raghavachari; J. B. Foresman; J. V. Ortiz; Q. Cui; A. G. Baboul; S. Clifford; J. Cioslowski; B. B. Stefanov; G. Liu; A. Liashenko; P. Piskorz; I. Komaromi; R. L. Martin; D. J. Fox; T. Keith; M. A. Al-Laham; C. Y. Peng; A. Nanayakkara; M. Challacombe; P. M. W. Gill; B. Johnson; W. Chen; M. W. Wong; C. Gonzalez; J. A. Pople, Gaussian 03; Revision B.03, Gaussian Inc.: Wallingford CT, 2004.
- [10] The Stuttgart relativistic small core basis set were obtained from the The Basis Set Exchange (BSE) version 1.2.2, as developed and distributed by the Environmental Molecular Sciences Laboratory. <https://bse.pnl.gov/bse/portal>: K. L. Schuchardt; B. T. Didier; T. Elsethagen; L. Sun; V. Gurumoorthi; J. Chase; J. Li; T. L. Windus, *J. Chem. Inf. Model.*, **2007**, *47*, 1045.
- [11] K. Wiberg, *Tetrahedron*, **1968**, *24*, 1083.
- [12] A. C. Malmborg, A. Michaëlsén, M. Ohlin, B. Jansson, and C.A.K. Borreback. *Scan. J. Immunol.*, **1992**, *35*, 643; (b) R. Karlsson, A. Miachaelsson, and L. Matsson, *J. Immunol. Methods*, **1991**, *145*, 229; (c) L.G. Fägerstam, Å. Frostell-Karlsson, R. Karlsson, B. Persson, and I. Rönnberg, *J. Chromatogr.* **1992**, *597*, 397.
- [13] T.A. Morton, D.G. Myszka, and I. Chaiken, *Anal. Biochem.* **1995**, *227*, 176.
- [14] K. Taewook, M. Jungwoo, O. Seogil, C. Soonwoo and Y. Jongheop; *Chem. Comm.* **2005**, 2360.
- [15] A. Caballero, R. Martinez, V. Lloveras, I. Ratera, J. Vidal-Gancedo, K. Wurst, A. Tarraga, P. Molina, J. Veciana, *J. Am. Chem. Soc.* **2005**, *127*, 15666.